Journal of Alloys and Compounds 509 (2011) 5677–5682

Contents lists available at ScienceDirect

Journal of Alloys and Compounds

journal homepage: www.elsevier.com/locate/jallcom

Preparation and characterization of visible light-driven AgCl/PPy photocatalyst

Shuna Gu, Bing Li, Chongjun Zhao*, Yunlong Xu, Xiuzhen Qian, Guorong Chen

Key Laboratory for Ultrafine Materials of Ministry of Education, Shanghai Key Laboratory of Advanced Polymeric Materials, School of Materials Science and Engineering, East China University of Science and Technology, Shanghai 200237, PR China

ARTICLE INFO

Article history:
Received 16 November 2010
Received in revised form 21 February 2011
Accepted 22 February 2011
Available online 1 March 2011

Keywords:
AgCl/PPy composites
AgCl
Visible light-driven photocatalysis
Photoreduction

ABSTRACT

Visible light photoactive AgCl/polypyrrole (PPy) composites were prepared via the reaction between excessive Ag^+ and Cl^- ions in the presence of PPy. The AgCl/PPy composites were systematically characterized using Fourier transform infrared (FTIR) spectroscopy, Raman spectra, X-ray diffraction (XRD), Scanning electron microscope (SEM), Transmission electron microscope (TEM) and Thermal gravity analysis (TGA). It was found that face-centered cubic AgCl nanocrystallite and 0.2 wt% PPy component existed in the composite and spherical AgCl/PPy nanoparticles were in the range of 200–600 nm. The AgCl/PPy composites showed higher visible light-driven photocatalytic activity and stability than that of AgCl. A photoreduction mechanism was postulated for AgCl/PPy photocatalyst on dye methyl orange (MO). The used AgCl/PPy photocatalyst was facilely regenerated by an oxidation process in aqueous $FeCl_3$ solution.

1. Introduction

Photocatalysis attracts much interest due to its potential applications in dealing with environmental pollution from photodegradation, producing new energy from photocatalyzed water splitting, and killing bacteria via photocatalytic destruction of microorganisms. Especially, the study on visible light photocatalysts has become one of the most important subjects for the development of photocatalysis under solar light, which consists of 43% visible light and only 4% UV light. To date, the spectra of the well-known UV photocatalyst TiO_2 has been extended from UV to visible region by doping approach [1,2], introducing disorder [3], modifying [4], or forming composites [5–7]. Alternatively, much more efforts have focused on to the development of new visible light-driven photocatalysts, e.g., $Bi_2Fe_4O_9$, Bi_2WO_6 and $CuO/BiVO_4$ composite [8–10].

Silver halides (AgXs) are well known photosensitive materials extensively applied as source materials in photography films, i.e., they are photoactive to both UV and visible light irradiation, in spite of their large bandgap, e.g., a direct bandgap of 5.15 eV (241 nm) and an indirect bandgap of 3.25 eV (382 nm) for AgCl. However, unwanted and uncontrolled photographic process of AgXs caused by photogenerated electrons (reduction process: $Ag^+ + e^- \rightarrow Ag^0$) under light irradiation inhabits pure AgXs to be directly used as stable photocatalysts. Therefore, a great number of attempts have been made to improve the photo-stability of silver halides by efficiently trapping photogenerated electrons and transferring them to oxidizing species. Firstly, some inert support including silica and zeolite had proved that it could stabilize the silver halides by preventing Ag^+ of silver halides from reducing to Ag^0. Secondly, similar promotion on photocatalytic stability of AgXs was also been observed when AgXs were used as co-photocatalyst with other semiconductors (SCs), e.g. TiO_2, H_2WO_4, $Ag_8W_4O_{16}$ or BiOI [11–15]. Thirdly, a facile and efficient meaning was to prepare the Ag/AgX composites by controllably reducing Ag^+ to Ag^0 on the surface of AgX particles during the synthesis process [16,17]. Stable photocatalysts including AgX/support composites [18], AgX/SC [19,14], or Ag/AgX [20–25] have been well used in the photodegradation of organic pollutants or reduction of heavy metal ions [26]. Furthermore, complex composites formed by immobilizing Ag/AgX on inert supports [27–29] and magnetic Fe_2O_3 [30] (Ag/AgX/suppport) or combining Ag/AgCl with other semiconductors (Ag/AgX/SC) [31] exhibited enhanced efficiency in photocatalytic degradation. In addition, these Ag/AgX/support and Ag/AgCl/SC composites also worked well in photocatalytic bactericide [32,33]. These indicate that Ag/AgXs play key roles in photocatalysis process both as a photocatalyst and a co-photocatalyst.

Inspired by the double effect of Ag^0 in Ag/AgXs in photocatalytic mechanism (trap and transfer photogenerated electrons, strongly harvest light in visible region [16,17,34]), it is postulated to develop an efficient and stable visible light-driven AgX composite photocatalyst by combining AgX with those materials having both good conductivity and strong optics absorption in visible region. In general, conducting polymers, especially polypyrrole (PPy) offer distinct UV absorption in visible light region with good conductivity. Therefore, AgX/CP composites have the potential to become a

* Corresponding author. Tel.: +86 21 6425 0838; fax: +86 21 6425 0838.
E-mail address: chongjunzhao@ecust.edu.cn (C. Zhao).

0925-8388/$ – see front matter © 2011 Elsevier B.V. All rights reserved.
doi:10.1016/j.jallcom.2011.02.121

new kind of active photocatalysts. Recently, composites of AgXs and conducting polymers (CPs) (AgX/CP) have prompted interest from several groups [35,36] while their application in visible light-driven photocatalysis is seldom reported to the best of our knowledge.

In the present report, we provided a facile synthesis method to prepare AgCl/PPy composites by adding Cl^- in an Ag/PPy colloid, which was used as the source of both PPy particles and Ag^+ ions [37]. The as-synthesized AgCl/PPy composite showed good photocatalytic activity under visible light irradiation, and the presence of PPy in AgCl/PPy significantly increased its durability. A possible photoelectron transfer mechanism was proposed on a basis of photodegradation performance, variation in UV–vis absorption spectra and SEM images before and after photocatalytic process.

2. Experimental details

2.1. Materials and reagents

$AgNO_3$ and DMF were purchased from Shanghai Chemical Reagent Co. Ltd. (Shanghai, China), and HCl was purchased from Sinopharm Chemical Reagent Co. Ltd. (Shanghai, China). Pyrrole was purchased from Acros. All these reagents were analytical grade reagents (A.R.) and used without further purifications.

2.2. Preparation of AgCl/PPy composite

Ag/PPy composites were synthesized according to the method described in our previous report [37]. The AgCl/PPy composite was prepared by adding concentrated HCl solution into the as-prepared Ag/PPy colloid (blue color). After the addition of HCl, the grey color AgCl/PPy composite precipitated from freshly prepared colloid. Alternatively, for DMF-diluted or aged colloid, the HCl-added Ag/PPy colloid was then added to the solvents including H_2O, EtOH or MeOH, and AgCl/PPy composite precipitated. After being washed with EtOH and dried in the air, grey AgCl/PPy composite powder was obtained. For comparison, pure AgCl was prepared under the same conditions except $AgNO_3$ solution instead of Ag/PPy colloid was used as the Ag^+ source.

2.3. Characterizations

UV–vis reflectance spectra of AgCl/PPy and AgCl powder were recorded on a Cary-500 spectrophotometer. Samples for Transmission Electron Microscopy (JEM-2010, JEOL) were prepared by dipping carbon-coated grids in the AgCl/PPy suspension, and the samples for SEM (S 4800, Hitachi) were prepared by sprinkling some AgCl or AgCl/PPy powder onto the surface of conducting adhesive tape. The samples for XRD patterns were obtained by evaporating drops of the AgCl or AgCl/PPy suspension on a silica or glass substrate. Thermal gravity analysis (TGA) of AgCl of AgCl/PPy was carried out with a Perkin-Elmer thermo gravimetric analyzer (TG-DTA, model SSC-5200, Seiko) at the temperature range of 40–700 °C under environment atmosphere. AgCl films were obtained when AgCl or AgCl/PPy powder sprinkled on silica sheet was heated up at a rate of 10 °C/min to 700 °C and kept for 2 h, and then cooled down to room temperature.

2.4. Photoactivity measurements

Catalytic and photocatalytic degradation of methyl orange (MO) dye was carried out with different dosages of the powdered photocatalyst (~0.05, 0.1, 0.15, 0.2 g) suspended in 25 mL of MO dye aqueous solution (20 mg/L) at room temperature in air. The optical system for detecting the photocatalytic reaction included a 350 W Xenon arc lamp with UV cutoff filter (providing visible light: $\lambda \geq 400$ nm). Prior to irradiation, the MO solution over the catalyst was kept in dark for 30 min to obtain the equilibrium adsorption state. The degradation of MO dye was monitored by UV/Vis absorption spectra (Spectrumlab 54 T UV–vis spectrophotometer, Lengguang Tech., Shanghai, China).

3. Results and discussion

3.1. Synthesis and dissolution-reprecipitation of AgCl/PPy composites

AgCl/PPy composites were facilely synthesized via adding HCl solution into the freshly prepared Ag/PPy colloids. The as-synthesized AgCl/PPy precipitation dissolved when it was added into a mixture solution of DMF and HCl, and the solubility of AgCl/PPy initially increased with the increase of volume content of HCl (until 15%) in DMF–HCl mixture solution, and then slightly decreased until 30% following a dramatic decrease at 40%. For comparison, the primary experiment demonstrated that the dissolution of AgCl/PPy was not observed in either pure DMF or concentrated HCl. On the other hand, when H_2O, EtOH or MeOH was added into the above AgCl-dissolved DMF–HCl solution, the AgCl/PPy precipitation was clearly observed.

Obviously, in the above precipitation and dissolution process of AgCl/PPy, HCl first supplied Cl^- for precipitation of AgCl/PPy in the presence of Ag^+ ions in Ag/PPy colloid, however, HCl also provided Cl^- for dissolution of AgCl/PPy, in which DMF acted as a unique medium for the accommodation of AgCl/PPy. Furthermore, not H^+ ions but Cl^- play a crucial role in dissolving the AgCl/PPy composite in DMF–HCl, for the similar complexes of both Ag-Br and Ag-I were also early reported with addition of not H^+ but bromide or iodide ions in DMF medium. The dissolution of AgCl/PPy in DMF in the presence of excess Cl^- was assumed to be attributed to the formation of complex of Ag-Cl, just like the corresponding complexes formed in the aqueous solution of $NH_3{\cdot}H_2O$, $Na_2S_2O_3$ and KCN. This Ag-Cl complex assumption was further confirmed by both appearance of the peak around 272 nm in the UV–vis absorption spectrum which was consistent with observation by Liu et al. [38]. The accommodation of AgCl/PPy in DMF + HCl, i.e., the stability of Ag-Cl/PPy complex strongly depended on the volume content of HCl and content of dissolved AgCl/PPy. In addition, the Ag-Cl/PPy complex was sensitive to the addition of protic solvents including H_2O, EtOH or MeOH. When one of these solvents was added, Ag-Cl complex was destroyed and AgCl/PPy precipitated. Similarly, the Ag-Cl complex was also destroyed and AgCl/PPy precipitation produced when the solvent DMF in complex solution was evaporated. The emergency of six characteristic crystalline peaks in the XRD patterns of AgCl/PPy film prepared by evaporating Ag-Cl complex solution at $2\theta = 27.8$, 32.24, 46.24, 54.82, 57.46 and 76.72° (not shown) (JCPDS no. 31-1238) partially supported the above hypothesis.

The above Ag-Cl complex could be well dispersed in several aprotic solvents including both non-polar solvents (CCl_4, CH_2Cl_2) and polar solvent (acetone). For comparison, Robert reported a silver halide soluble in various organic solvents by capping silver halides with an organic material layer with metal ion handles, respectively [39]. The solubility of Ag-Cl complex in organic aprotic solvents may be useful in preparing organic AgCl solution or colloid, which supplies a way to incorporate photochromic AgX into a polymer matrix, especially those transparent polymers, e.g., poly(methyl methacrylate) (PMMA), polycarbonate (PC) for some optical uses [39].

3.2. FTIR, Raman spectra, and XRD patterns of as-synthesized AgCl/PPy composites

Presence of PPy component in AgCl/PPy was confirmed by both FTIR and Raman spectra. As shown in Fig. 1, the spectrum for pure PPy exhibits the characteristic absorption bands at 1548, 1470, 1298, 784 and 678 cm^{-1}. They are assigned to pyrrole ring stretch, =C—H in-plane deformation and C—H outer-bending vibrations, respectively, and is well consistent with the reported bands [40]. These bands also appear in the FTIR spectrum for AgCl/PPy sample, curve b (1544, 1461, 1284, 782, 674 cm^{-1}), implying the formation of PPy backbone chains. Furthermore, these characteristic bands became weakened and shifted to lower wavenumbers in the spectrum of the composite, which might due to the low concentration of PPy as well as the possible interplay of PPy with AgCl in the composites. The existence of PPy in the AgCl/PPy composite was further confirmed by the typical absorbance in Raman spectrum at 1580, 1380, 1245, 1105, and 945 cm^{-1} (not shown), which correspond to polypyrrole, ring CC, CN stretch, symmetrical C—H in-plane bend, and ring deformation, respectively [41].

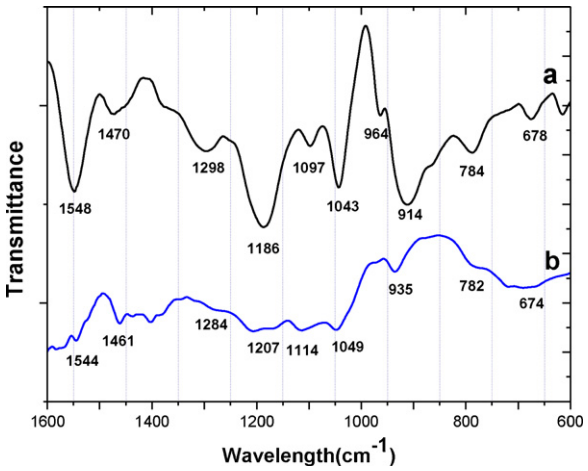

Fig. 1. FTIR spectra of (a) pure PPy powder and (b) AgCl/PPy composite powder.

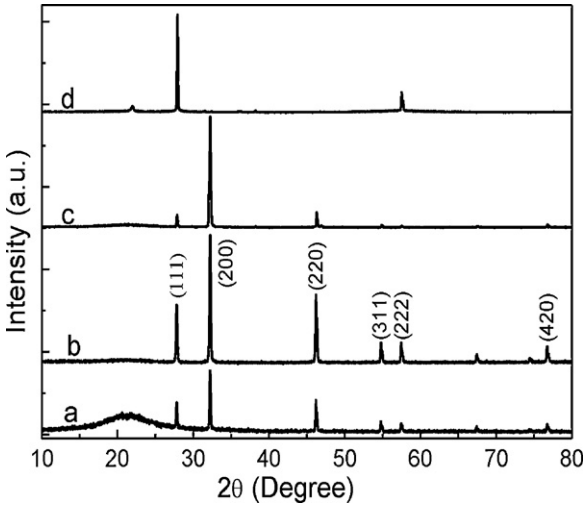

Fig. 2. XRD patterns of (a) AgCl/PPy as-synthesized, (b) AgCl/PPy and AgCl annealed, anneal conditions: 700 °C for 2.0 h.

As CPs content burned out at temperatures above 600 °C, the relative content of PPy in the AgCl/PPy composite could be obtained by calculating the weight loss in TGA method at a temperature over 600 °C, and it was ca. 0.2% (650 °C).

XRD patterns of AgCl/PPy powder were carried out to investigate the composite crystal phase. Curve a and b in Fig. 2 correspond to the XRD patterns of AgCl/PPy powder obtained by reacting HCl with $AgNO_3$ solution and Ag/PPy colloid, respectively. Peaks at $2\theta = 27.86$, 32.24, 46.24, 54.82, 57.46 and 76.72° can be indexed as (1 1 1), (2 0 0), (2 2 0), (3 1 1), (2 2 2) and (4 2 0) reflection lines of face-centered cubic AgCl (JCPDS no. 31-1238). It is noted that no peaks corresponding to elemental Ag were discerned. Combining the XRD results with the FTIR and Raman observations, we can conclude that AgCl/PPy composites were obtained. Compared with the XRD pattern of pure AgCl (curve b), no distinct difference was observed. In other words, the introduction of PPy content changed the XRD patterns of AgCl/PPy little, although it effectively affected the orientation preference of AgCl/PPy. Solid AgCl film prepared by annealing AgCl/PPy powder at 700 °C exhibited the strongest peak at (1 1 1) plane instead of original (2 0 0), but that from AgCl powder kept unchanged (2 0 0) plane, while other peaks except maximum one dramatically decreased for both powder, as shown in curve c and curve d of Fig. 2. Tunable properties of crystal plane might exploit the application of this AgCl or its composites. As no same effect was observed in the mixture powder of AgCl and pure PPy, this crystal plane tuning properties might be attributed to a strong interaction between AgCl and PPy.

3.3. SEM and TEM images of as-synthesized AgCl/PPy composites

Fig. 3A shows the SEM images of AgCl/PPy synthesized by adding concentrated HCl solution to a freshly prepared Ag/PPy colloid. It is clearly seen that except some large nearly cuboid particles with the size of ca. 1 μm or more, most of the particles are in the range from 200 nm to 600 nm. For a comparison, most large compact particles, which show the size of ca. 1 μm or more (Fig. 3B), accompanied by a small amount of smaller particles with the size of hundreds of nanometers, were formed for pure AgCl samples. Obviously, this distinctly difference in size between AgCl/PPy and AgCl was attributed to the different state of Ag^+ precursor: Free Ag^+ in $AgNO_3$ solution (for pure AgCl), and limited Ag^+ by as-synthesized PPy in Ag/PPy colloid (for AgCl/PPy composite). This evidence indicates that the existence of PPy, although only 0.2% concentration, distinctly decreased the size of AgCl particles. The insets in Fig. 3A and B give the typical TEM images of AgCl/PPy and pure AgCl, respectively. It is clearly seen that for AgCl/PPy the particles are adhered by some amorphous substance, while for AgCl the particles are well separated, confirming the existence of PPy layer on the surface or nearby the AgCl particles for AgCl/PPy samples.

3.4. Photocatalytic performance of AgCl/PPy powder

Fig. 4 shows the typical UV–vis diffuse reflectance spectra of the as-synthesized AgCl powder (curve a) and AgCl/PPy composite powder (curve b). It is clearly seen that in the visible and near-IR regions there is no distinct absorption band for the pure AgCl powder (curve a, Fig. 4), which is similar to the results reported [13,16,23]. On the other hand, the AgCl/PPy composite powder shows a broad absorption band ranging from 400 nm to 500 nm

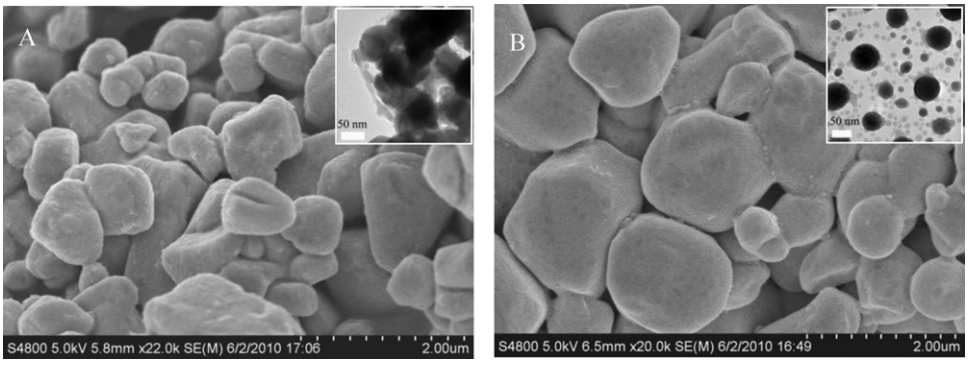

Fig. 3. SEM images of AgCl/PPy composites (A), and AgCl (B) as-synthesized. The inset: TEM image of AgCl/PPy composite (A), TEM image of AgCl (B).

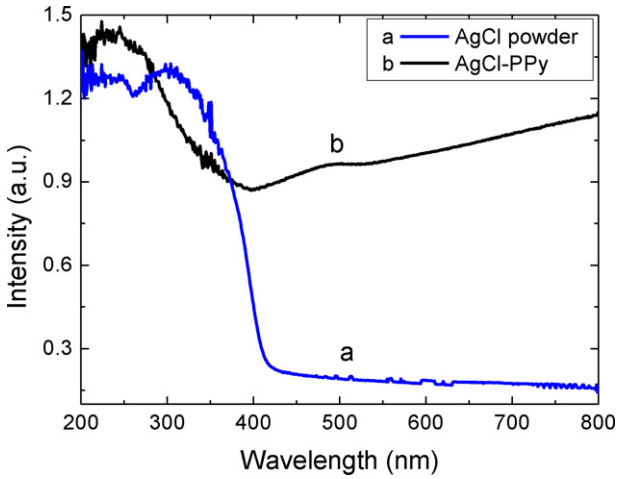

Fig. 4. UV–vis reflectance spectra of (a) AgCl powder, (b) AgCl/PPy powder.

and centered at 489 nm as well as an absorption tail (curve b, Fig. 4), which are characteristic of doped and highly conductive PPy [42]. These evidences indicate that the presence of PPy component strongly enhanced the absorption in visible and near-infra region, which might be favor the enhancement of the visible light photocatalytic activity of AgCl/PPy composite.

Decomposition experiments were carried out by dispersing AgCl/PPy powder samples in MO aqueous solutions, which were under agitation and irradiated by light-filtered ($\lambda \geq 400$ nm) Xenon arc lamp light. Fig. 5A gives the degradation efficiency of MO as a function of irradiation time, and the absorption spectra data of the sample solution was obtained every 3 min interval. It was clearly observed that the sample solution quickly bleached, and entirely degraded in 15 min. Especially for AgCl/PPy photocatalyst, MO was almost completely degraded within 6 min at the initial 3 cycles. Although the photocatalytic efficiency of AgCl powder was comparable to that of AgCl/PPy powder at the 1st cycles, it quickly weaken with the running cycles, e.g., at 5th cycle, degradation rate of MO for AgCl photocatalyst was distinctly lower than that for AgCl/PPy (30% vs. 50% at 3rd min).

To test the recyclability of MO bleaching on AgCl/PPy, we repeated the 15 min bleaching experiment for 10 times using 0.15 g photocatalyst under visible light irradiation. As shown in Fig. 5B, MO dye was quickly bleached after every injection of the MO solution, and the photocatalyst AgCl/PPy was stable under repeated use with nearly constant photodecomposition rate. For example, ca. 98% photodegradation was obtained at 10th cycle for AgCl/PPy powder sample, while only about 58% was obtained at 10th cycle for AgCl powder.

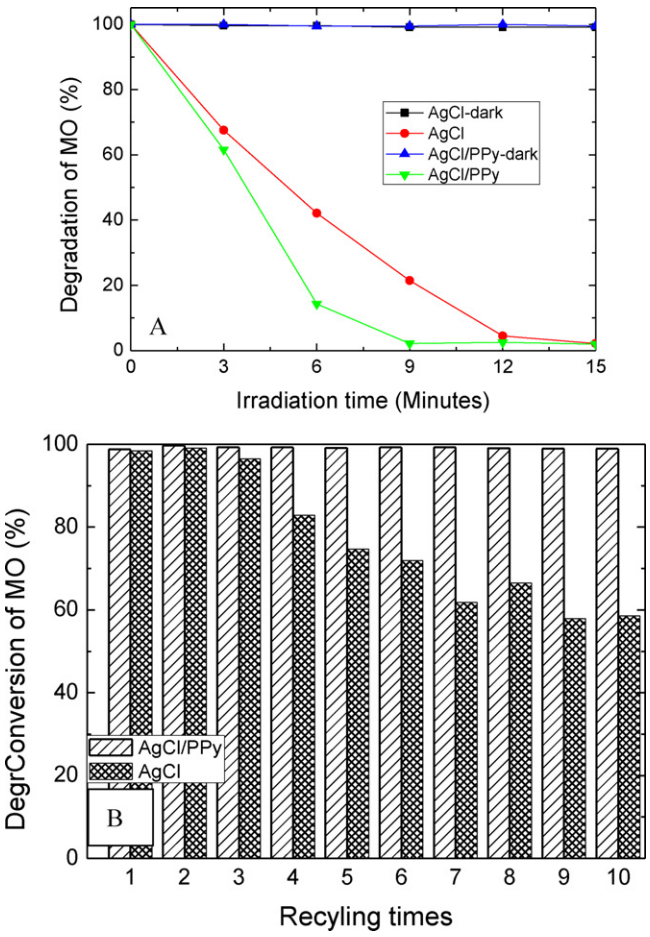

Fig. 5. (A) Photodegradation of MO dye in solution as a function of irradiation time over AgCl/PPy and AgCl catalyst at 0.15 g, (B) cycling runs of MO degradation in the presence of catalyst AgCl/PPy (0.15 g) under visible light irradiation.

Degradation experiments in the dark with AgCl/PPy (catalysis) and under light irradiation without photocatalyst (photolysis) were carried out to investigate the fact that the decomposition of MO dye upon AgCl/PPy was not attributed to either catalysis or photolysis. As shown in Fig. 5A, no change was observed when the photocatalysis processes were carried out in the absence of either AgCl/PPy or light irradiation. This confirms that AgCl/PPy composite is an active visible light-driven photocatalyst.

Fig. 6A and B show the SEM graphs of AgCl/PPy and AgCl subjected to 10-cycle photoirradiation process under visible light irradiation, respectively. Compared with the sample as-prepared

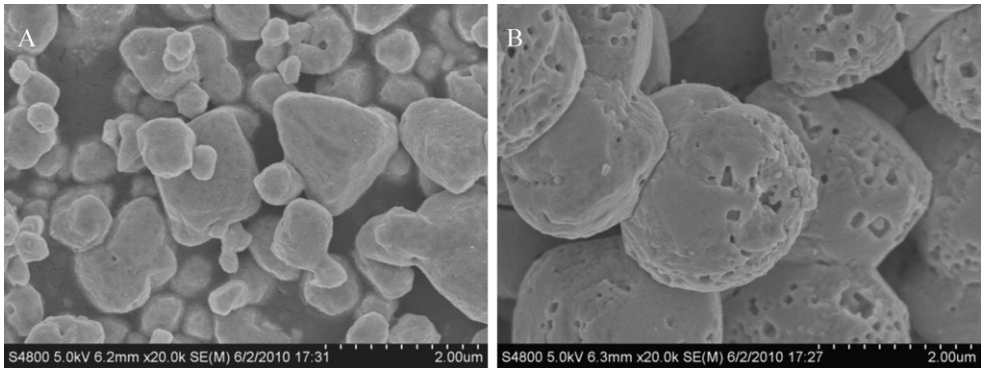

Fig. 6. SEM images of AgCl/PPy composites (A), and AgCl (B) used for 10 cycles.

AgCl powder, two changes were observed for used AgCl sample, shown in Fig. 6B. First, the appearance of many corroded holes formed on the AgCl particles surface. Secondly, the disappearance of those smaller particles with sub-micrometers was correlated with continuous reduction of AgCl caused by its photosensitivity. In the case of AgCl/PPy (Fig. 6A), it is clearly observed that no corrosion hole was produced on the particles surface. Moreover, the smaller particles still existed, i.e., the transformation of AgCl to Ag^0 was efficiently inhibited. These comparison results indicate that the PPy played an important role in keeping the photostability of AgCl in the AgCl/PPy composite under visible light irradiation.

Another controlled experiment was carried out in order to further elaborate the effect of PPy content on the photoactivity of AgCl/PPy. When the Ag/PPy prepared under identical conditions except the addition of a little bit $NH_3{\cdot}H_2O$, since the base solution decreased both the electroactivity and conductivity of PPy, the AgCl/PPy prepared using this kind of Ag/PPy showed less photocatalytic performance under the visible light indicating lower activity.

3.5. Mechanism involved in the photocatalytic degradation

The mechanism involved in the photocatalytic process of AgX to dye MO was previously investigated by different groups [16,43,44]. There were some discrepancies, e.g., Huang and co-workers [16] and Hu et al. [43] attributed photocatalytic degradation of MO to a photooxidation process, while Zang et al. [44] regarded the photodegradation process as a photoreduction process. Moreover, Zang et al. identified that a new peak appeared around 247 nm and grew until MO completely degraded, which was assigned to the reduction product of MO, hydrazine derivative [45]. The product from MO oxidation, amine oxide derivatives [46] characteristic of an absorption peak at 320 nm was not observed. As shown in curve a–f in Fig. 7, there is no distinct absorption band around 320 nm that can be attributed to the amine oxide derivatives observable for AgCl/PPy photocatalyst. Absorption peak at 270 nm becomes diminished and a new peak at 247 nm appears and increases with increasing of irradiation time. These indicate that photoreduction of MO involved both AgCl and AgCl/PPy catalyst in this work, irrespective of the fact that no zeolite participated.

It is known that AgCl owns both high direct band gap (5.6 eV) and indirect band gap (3.25 eV). However, it is photosensitive because of its point ionic defects and electron traps, and thus it is continuously and irreversibly converted into Ag^0 and subsequently aggregates to form Ag cluster or particles under visible light irradiation, which hinders the application of AgCl or other AgX as a stable photocatalyst. Recently, Ag/AgX composites attracted the attention of many researchers owing to their good stability and high efficiency. Refereeing to the stability of Ag/AgCl, Hu et al. [43] and Huang and co-workers [16] attributed the photocatalyst stability of AgX composite to the photogenerated electrons which were not transferred to the Ag^+ ions of the AgCl lattice but trapped by the Ag NPs, and then by the adsorbed O_2 in the solution to form superoxide ion (O_2^-) and other reactive oxygen species [47]. In our work, although no Ag^0 was involved, its good conductivity facilitates PPy to substitute for Ag^0 to trap and transfer photogenerated electrons so as to inhibit the reduction of AgCl by photogenerated electrons. In this way, the stability of photocatalyst AgCl/PPy was enhanced. This conjecture was further confirmed by the higher photoactive efficiency and stability for AgCl/PPy than that for AgCl in the photodegradation experiment (Fig. 5A and B), as well as slighter corrosion in the SEM results (Fig. 6A and B).

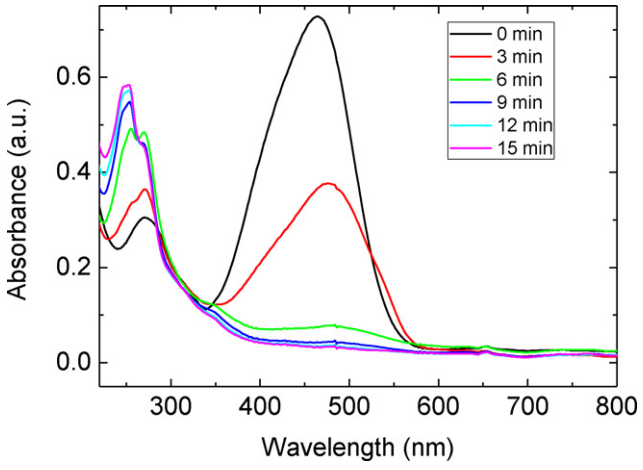

Fig. 7. Variation of UV–vis absorbance of MO with times, photocatalyst: 0.15 g AgCl/PPy.

According to the photoreduction property and key role of PPy for AgCl/PPy photocatalyst, and combining with the mechanism in references [16,43,44], we propose a simple charge carriers (electrons or holes) transfer route. After photogenerated by photoactive AgCl, electrons were trapped by conductive PPy and thus separated from its hole pair (Eq. (1)), and then rapidly transferred by PPy to the adsorbed O_2 to form the active reduction products, e.g., O_2^- (Eqs. (2) and (3)), and then these reduction products (O_2^- or e^-) photodegraded the dye MO (Eq. (4)). On the other hand, hole was scavenged by Cl^- to form active oxidation production Cl^0 [16] (Eq. (5)) or trapped by the basic sites to lose the oxidation capacity [44]. However, contribution of the oxidation production Cl^0 to the degradation of MO (Eq. (6)) was minor, for the absorption band around 320 nm corresponding to the amine oxide derivative [46] was not identified.

$$AgCl \xrightarrow{h\nu} e^- + h^+ \quad (1)$$

$$PPy + e^- \rightarrow PPy - e^- \quad (2)$$

$$PPy - e^- + O_2 \rightarrow O_2^- + PPy \quad (3)$$

$$MO + O_2^- (\text{or } e^-) \rightarrow \text{hydrazine derivate} + O_2 \quad (4)$$

$$h^+ + Cl^- \rightarrow Cl^0 \quad (5)$$

$$MO + Cl^0 (\text{or } h^+) \rightarrow \text{amine oxide derivative} \quad (6)$$

3.6. Regeneration of AgCl photocatalyst

Due to the photosensitivity, which causes the uncontrolled transformation of photoactive AgCl into Ag^0, AgCl becomes inactive after some cycles (e.g. 15 times). If a method could be used to re-transform the Ag^0 into AgCl, photoactivity of these AgX photocatalyst would be refreshed or regenerated. A chemical redox reaction between $FeCl_3$ and Ag had been used to convert Ag nanowire into Ag/AgCl nanowire, giving these composite nanowire good photocatalysis degradation on MO dyes [48]. It was found that when the inactive AgCl/PPy or AgCl photocatalyst after ten times cycling of irradiation was treated in aqueous $FeCl_3$ solution, the photocatalyst partially recovered its photocatalytic activity on MO dye again.

4. Conclusions

A facile method to prepare AgCl/PPy composites was developed via reaction of Ag^+ in Ag/PPy colloid and Cl^-. The presence of PPy decreased the size of AgCl particles down to nanometer scale, and tailored the crystal plane formation during annealing. Under visible light irradiation, the AgCl/PPy composites exhibited highly efficient and stable photocatalytic properties on MO, following photoreduction mechanisms. In a perspective, the method to produce AgCl/PPy

composites can be extended to other photocatalysts of AgX/PPy composites, such as AgBr/PPy or AgI/PPy.

Acknowledgments

The authors thank Prof. Kake Zhu for in depth discussions. We are grateful for the support from the National Natural Science Foundation of China (no. 20504026, 20604015), International Scientific and Technological Cooperation Program of Shanghai (no. 08230705600), and Shanghai Nanotechnology Promotion Center (no. 0852nm02300), Shanghai Leading Academic Discipline Project (B502) and Shanghai Key Laboratory Project (08DZ2230500).

References

[1] C.M. Tech, A.R. Mohamed, J. Alloys Compd. 509 (2011) 1648–1660.
[2] J. Zheng, Z.Q. Liu, X. Liu, X. Yan, D.D. Li, W. Chu, J. Alloys Compd. 509 (2011) 3771–3776.
[3] X.B. Chen, L. Liu, P.Y. Yu, S.S. Mao, Science 331 (2011) 746–750.
[4] L. Baia, L. Diamandescu, L. Barbu-Tudoran, A. Peter, G. Melinte, V. Danciu, M. Baia, J. Alloys Compd. 509 (2011) 2672–2678.
[5] Y.D. Liu, F. Xin, F.M. Wang, S.X. Luo, X.H. Yin, J. Alloys Compd. 498 (2010) 179–184.
[6] Y. Liu, J.C. Hu, J.L. Li, J. Alloys Compd. 509 (2011) 2434–2440.
[7] H.J. Yan, H.X. Yang, J. Alloys Compd. 509 (2011) L26–L29.
[8] M. Zhang, H. Yang, T. Xian, Z.Q. Wei, J.L. Jiang, Y.C. Feng, X.Q. Liu, J. Alloys Compd. 509 (2011) 809–812.
[9] Y. Tian, G.M. Hua, W. Xu, N. Li, M. Fang, L.D. Zhang, J. Alloys Compd. 509 (2011) 724–730.
[10] C.L. Yu, K. Yang, J.C. Yu, F.F. Cao, X. Li, X.C. Zhou, J. Alloys Compd. (2011) 100, doi:10.1016/j.jallcom.2011.01.
[11] Y.J. Zang, R. Farnood, Appl. Catal. B 79 (2008) 334–340.
[12] C. Hu, J. Guo, J.H. Qu, X.X. Hu, Langmuir 23 (2007) 4982–4987.
[13] P. Wang, B.B. Huang, X.Y. Zhang, X.Y. Qin, Y. Dai, H. Jin, J.Y. Wei, M.-H. Whangbo, Chem. Eur. J. 14 (2008) 10543–10546.
[14] H.F. Cheng, B.B. Huang, Y. Dai, X.Y. Qin, X.Y. Zhang, Langmuir 26 (2010) 6618–6624.
[15] X.F. Wang, S.F. Li, H.G. Yu, J.G. Yu, J. Mol. Catal. A 334 (2011) 52–59.
[16] P. Wang, B.B. Huang, X.Y. Qin, X.Y. Zhang, Y. Dai, J.Y. Wei, M.-H. Whangbo, Angew. Chem. Int. Ed. 47 (2008) 7931–7933.
[17] P. Wang, B.B. Huang, X.Y. Zhang, X.Y. Qin, H. Jin, Y. Dai, Z.Y. Wang, J.Y. Wei, J. Zhan, S.Y. Wang, J.P. Wang, M.-H. Whangbo, Chem. Eur. J. 15 (2009) 1821–1824.
[18] A. Pourahmad, Sh. Sohrabnezhad, E. Kashefian, Spectrochim. Acta A 77 (2010) 1108–1114.
[19] P.W. Huo, Y.S. Yan, S.T. Li, H.M. Li, W.H. Huang, Desalination 256 (2010) 196–200.
[20] P. Wang, B.B. Huang, X.Y. Zhang, X.Y. Qin, Y. Dai, Z.Y. Wang, Z.Z. Lou, ChemCatChem 3 (2011) 360–364.
[21] H. Xu, H.M. Li, J.X. Xia, S. Yin, Z.J. Luo, L. Liu, L. Xu, ACS Appl. Mater. Inter. 3 (2011) 22–29.
[22] C.H. An, S. Peng, Y.G. Sun, Adv. Mater. 22 (2010) 2570–2574.
[23] Y.Y. Li, Y. Ding, J. Phys. Chem. C 114 (2010) 3175–3179.
[24] M.J. Choi, K.-H. Shin, J. Jang, J. Colloid Interface Sci. 341 (2010) 83–87.
[25] P. Wang, B.B. Huang, Z.Z. Lou, X.Y. Zhang, X.Y. Qin, Y. Dai, Z.K. Zheng, X.N. Wang, Chem. Eur. J. 16 (2010) 538–544.
[26] P. Wang, B.B. Huang, Q.Q. Zhang, X.Y. Zhang, X.Y. Qin, Y. Dai, J. Zhan, J.G. Yu, H.X. Liu, Z.Z. Lou, Chem. Eur. J. 16 (2010) 10042–10047.
[27] C. Hu, T.W. Peng, X.X. Hu, Y.L. Nie, X.F. Zhou, J.H. Qu, H. He, J. Am. Chem. Soc. 132 (2010) 857–862.
[28] X.F. Zhou, C. Hu, X.X. Hu, T.W. Peng, J.H. Qu, J. Phys. Chem. C 114 (2010) 2746–2750.
[29] J.F. Guo, B.W. Ma, A.Y. Yin, K.N. Fan, W.L. Dai, Appl. Catal. B 101 (2011) 580–586.
[30] G.T. Li, K.H. Wong, X.W. Zhang, C. Hu, J.C. Yu, R.C.Y. Chan, P.K. Wong, Chemosphere 76 (9) (2009) 1185–1191.
[31] Y.G. Xu, H. Xu, H.M. Li, J.X. Xia, C.T. Liu, L. Liu, J. Alloys Compd. 509 (2011) 3286–3292.
[32] X.X. Hu, C. Hu, T.W. Peng, X.F. Zhou, J.H. Qu, Environ. Sci. Technol. 44 (2010) 7058–7062.
[33] L.S. Zhang, K.H. Wong, H.Y. Yip, C. Hu, J.C. Yu, C.Y. Chan, P.K. Wong, Environ. Sci. Technol. 44 (2010) 1392–1398.
[34] L. Kuai, B.Y. Geng, X.T. Chen, Y.Y. Zhao, Y.C. Luo, Langmuir 26 (2010) 18723–18727.
[35] Y.Y. Wei, Y. Zhao, L. Li, Liang, Yang X.M., X.H. Yu, G.P. Yan, Adv. Technol. 21 (2010) 742–745.
[36] Q. Zhang, F.J. Liu, L. Li, G.L. Pan, S.M. Shang, J. Nanopart. Res. 13 (2011) 415–421.
[37] C.J. Zhao, Q.T. Zhao, Q.Z. Zhao, J.R. Qiu, C.S. Zhu, J. Photochem. Photobiol. A 187 (2007) 146–151.
[38] C.Y. Liu, X.Y. Chen, Y.J. Wang, Chin. J. Chem. Phys. 10 (1997) 43–48.
[39] E.S. Robert, B.S. Kevin, US Patent 5252450, 1993-10-12.
[40] Q.L. Cheng, V. Pavlinek, A. Lengalova, C.Z. Li, Y. He, P. Saha, Microporous Mesoporous Mater. 93 (2006) 263–269.
[41] J.-Y. Kim, J.-T. Kim, E.-A. Song, Y.-K. Min, H.-o Mamaguchi, Macromolecules 41 (2008) 2886–2889.
[42] K.G. Neoh, T. Young, N.T. Looi, E.T. Kang, Chem. Mater. 9 (1997) 2906–2912.
[43] C. Hu, Y.Q. Lan, J.H. Qu, X.X. Hu, A.M. Wang, J. Phys. Chem. B 110 (2006) 4066–4072.
[44] Y.J. Zang, R. Farnood, J. Currie, Chem. Eng. Sci. 64 (2009) 2881–2886.
[45] S. Anandan, M. Yoon, J. Photochem. Photobiol. C 4 (2003) 5–18.
[46] J. Oakes, P. Gratton, J. Chem. Soc. Perkin Trans. 2 (1998) 2563–2568.
[47] M.R. Hoffmann, S.T. Martin, W. Choi, D.W. Bahnemann, Chem. Rev. 95 (1995) 69–96.
[48] Y.G. Sun, J. Phys. Chem. C 114 (2010) 2127–2133.